Chemical Engineering Journal 165 (2010) 846–850

Contents lists available at ScienceDirect

Chemical Engineering Journal

journal homepage: www.elsevier.com/locate/cej

Original article

Stability of Co–Ce–Mn mixed-oxide catalysts for CO preferential oxidation in H_2-rich gases

Qiang Guo, Shunquan Chen, Yuan Liu*, Yaquan Wang

Tianjin Key Laboratory of Applied Catalysis Science and Engineering, School of Chemical Engineering and Technology, Tianjin University, Tianjin 300072, China

ARTICLE INFO

Article history:
Received 15 March 2010
Received in revised form 6 October 2010
Accepted 12 October 2010

Keywords:
Carbon monoxide
Preferential oxidation
Deactivation
Carbon dioxide
Cobalt
Ceria
Manganese
Oxidation state

ABSTRACT

The stability of Co–Ce–Mn mixed-oxide catalysts for CO preferential oxidation in H_2-rich gases was investigated. The deactivation mechanism was explored using Fourier-transform infrared spectroscopy (FTIR), temperature-programmed desorption (TPD), and reduction and oxidation techniques. The deactivation of the catalysts was observed in reaction gas streams containing CO_2. FTIR and CO_2-TPD revealed carbonate formation in the deactivated samples. The activity of the deactivated catalysts could be partially regenerated by CO_2 desorption and fully regenerated by oxidation treatment which led to a change in the oxidation state of cobalt ions. It is proposed that both carbonate accumulation and the change in the oxidation state of cobalt ions during CO preferential oxidation are responsible for the deactivation of Co–Ce–Mn catalysts.

1. Introduction

Carbon monoxide must be removed from H_2-rich hydrocarbon gases used as the hydrogen source for fuel cells. H_2-rich gases produced by steam or autothermal reforming of hydrocarbons followed by the water–gas shift reaction contain approximately 1 vol.% CO. Fuel-cell anodes are highly sensitive to trace mounts of CO, resultantly the CO content needs to be purified to less than 10 ppm or less than 100 ppm for CO-resistant anodes [1–5]. Among different methods used to remove CO from H_2-rich gases, CO preferential oxidation (CO-PROX) is considered as the simplest and most effective one [6].

Cobalt oxide catalysts show high activity for CO-PROX in H_2-rich gases and for low-temperature CO oxidation [7–15]. We found that Co_3O_4–CeO_2 and Co_3O_4–CeO_2–MnO_x catalysts exhibited good catalytic performance for CO-PROX in H_2-rich gases and could completely remove CO from H_2-rich gases at ~170 °C [8,9]. Wang et al. [11] reported that pure Co_3O_4 catalysts showed high activity for CO oxidation at room temperature. Shao et al. [12] and our research group [14] confirmed that 100% CO conversion could be obtained at −70 °C over Co_3O_4/CeO_2 and manganese-doped Co_3O_4/CeO_2 catalysts with a small Co_3O_4 particle size, respectively. However, cobalt oxide catalysts show relatively poor stability for CO oxidation and CO-PROX, which limits their application. The deactivation of cobalt-based oxide catalysts for CO oxidation is generally attributed to the presence of water or the accumulation of carbonate species [16–20]. Jansson et al. proposed another hypothesis and suggested that the deactivation of cobalt oxide-based catalysts was caused by a change in graphite, since neither the formation of surface carbonates nor the irreversible reduction of Co^{n+} could explain their deactivation [21].

More detailed studies of the deactivation mechanism for cobalt oxide catalysts during CO-PROX are needed for improving catalytic performance and for the design of new stable catalysts. The objective of the present study is to further investigate the catalyst deactivation and regeneration mechanisms for Co_3O_4–CeO_2–MnO_x catalysts during CO-PROX.

2. Experimental

2.1. Catalyst preparation

Co_3O_4–CeO_2–MnO_x catalysts were prepared by co-precipitation as previously described [9]. Aqueous solutions of $Ce(NO_3)_3{\cdot}6H_2O$, $Co(NO_3)_2{\cdot}6H_2O$, and $Mn(NO_3)_2{\cdot}6H_2O$ were mixed at a molar ratio of 8:1:1. The mixed solution and a sodium carbonate solution were then gradually and simultaneously dropped into a continuously stirred flask at pH 8.5–9.5. After an aging period of 4 h, the resulting precipitate was filtered and washed with hot water until no change

* Corresponding author. Tel.: +86 022 87401675; fax: +86 022 87401675.
E-mail addresses: yuanliu@tju.edu.cn, llwinwill@163.com, leilei_112@yahoo.com.cn (Y. Liu).

1385-8947/$ – see front matter © 2010 Elsevier B.V. All rights reserved.
doi:10.1016/j.cej.2010.10.029

in pH was observed. The sample was dried in static air at 80 °C for 24 h and calcined at 350 °C for 5 h. Catalysts prepared in this way are denoted as Co–Ce–Mn.

2.2. Catalytic performance

The catalytic performance was tested in a fixed-bed flow reactor system consisting of a vertical quartz tube reactor (8 mm inner diameter) placed in an oven, where the temperature could be controlled between room temperature and 800 °C. The temperature was measured with thermocouples in the reactor bed. The samples were sieved to 40–60 mesh so that pressure drop and concentration and temperature gradients over the catalyst bed were negligible. 150 mg of catalysts was used for each run. The flow rates of reaction gases were controlled by Brooks mass flow meters. The reaction gas mixture consisted of 1 vol.% CO, 1 vol.% O_2, 50 vol.% H_2, 20 vol.% CO_2, 10 vol.% H_2O and N_2 (balance), and the space velocity was 80,000 ml h^{-1} $g_{cat}{}^{-1}$. H_2O was pumped to the reactor system by SP-500 micro infusion pump (JMS, Japan). Before each test, the Co–Ce–Mn catalyst was firstly oxidized with a gas mixture of 5 vol.% O_2/N_2 at 300 °C for 40 min on-line. The reactor was then cooled to the reaction temperature of 170 °C and the CO-PROX reaction tests were initiated.

To investigate the influence of H_2, CO_2 and H_2O on CO conversion, H_2, CO_2 or H_2O in the feeding gases was replaced by N_2, respectively.

The influence of pretreatment of Co–Ce–Mn catalysts on CO-PROX activity was investigated as follows. In the pre-oxidation cases, the catalysts were pretreated with a gas mixture of 5 vol.% O_2/N_2 at 300 °C for 40 min. In the pre-reduction cases, the samples were pretreated with a gas mixture of 5 vol.% H_2/Ar at 300 °C for 40 min. After pretreatment, the reactor was cooled to room temperature in N_2. The samples were then treated in a flow of CO_2 or N_2 at room temperature for 60 min and the temperature was then increased to 170 °C. Finally, CO_2 or N_2 was replaced by the reaction gas mixture as described above, and variations in CO conversion with reaction time were measured.

The outlet gas from the reactor was analyzed on a gas chromatography system equipped with thermal conductivity and flame ionization detectors. A nickel catalytic converter was used to detect trace amounts (<10 ppm) of CO.

2.3. Characterization

Fourier-transform infrared (FTIR) spectra were recorded on a Nicolet Nexus spectrometer over the range of 4000–400 cm^{-1}. The samples were diluted with KBr at a ratio of about 1:200 before tests, and the mixtures were then ground to a fine powder using an agate mortar and pestle. After finely mixed, the diluted samples were compressed into tablet form. Then, the tablets were put on a holder for FTIR spectral measurement.

CO_2 temperature-programmed desorption (CO_2-TPD) tests were conducted in a fixed-bed flow reactor. Before each test, fresh or pre-reduced catalyst samples (reduced at 300 °C for 30 min) were treated in flowing CO_2 at room temperature for 1 h. For CO_2-TPD tests on deactivated catalysts, no CO_2 pretreatment was performed and only He was introduced into the CO_2-TPD system. CO_2-TPD profiles were obtained by heating the samples from room temperature to 700 °C at 10 °C/min.

TPR and temperature-programmed oxidation (TPO) experiments were performed in a micro-flow reactor using samples of 50 mg. Prior to each TPR test, the samples were outgassed with N_2 at 40 °C for 30 min. H_2-TPR experiments then were performed at a heating rate of 10 °C/min from 40 to 900 °C in 5 vol.% H_2/Ar at a flow rate of 30 ml/min. Prior to each TPO test, the samples were pre-reduced at 300 °C for 40 min, then cooled to 40 °C in an N_2 flow. TPO profiles were obtained by measuring the amount of O_2 consumed when the temperature was increased from 40 to 600 °C at 10 °C/min under a flow of 5 vol.% O_2/He at 30 ml/min.

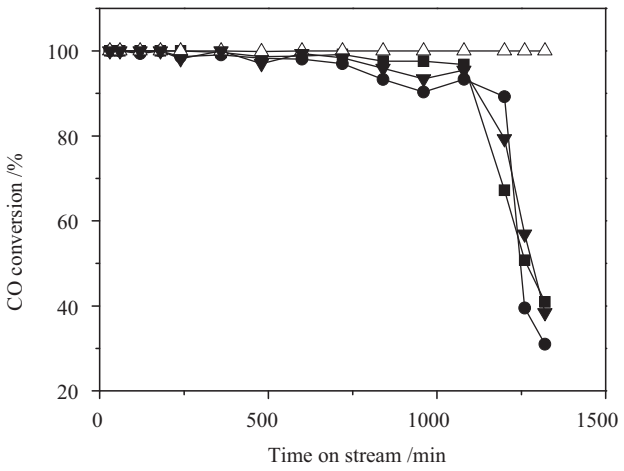

Fig. 1. Variation of CO conversion with reaction time over Co–Ce–Mn catalysts at 170 °C under the space velocity of 80,000 ml h^{-1} $g_{cat}{}^{-1}$ and in reaction gases of (■) 1 vol.% CO, 1 vol.% O_2, 50 vol.% H_2, 20 vol.% CO_2, 10 vol.% H_2O and N_2; (●) 1 vol.% CO, 1 vol.% O_2, 20 vol.% CO_2, 10 vol.% H_2O and N_2; (△) 1 vol.% CO, 1 vol.% O_2, 50 vol.% H_2, 10 vol.% H_2O and N_2; (▼)1 vol.% CO, 1 vol.% O_2, 50 vol.% H_2, 20 vol.% CO_2 and N_2.

3. Results

3.1. Influence of H_2, CO_2 and H_2O on catalyst activity

Since H_2, CO_2 or H_2O in the feed gases may influence CO oxidation over cobalt oxide or other transition metal oxides, their influence was investigated by changing the components of the reaction gas. Fig. 1 shows the variation in CO conversion with reaction time over Co–Ce–Mn catalysts for CO-PROX using different feed gases. When the reaction gas contained CO_2, regardless of whether H_2 and/or H_2O were present, CO conversion decreased with the reaction time with a similar trend over Co–Ce–Mn catalysts. CO conversion rapidly decreased after ~1100 min and the catalytic activity was almost completely lost after ~1400 min. By contrast, when the feed gas did not contain CO_2, 100% CO conversion was achieved throughout the reaction time, even though the gas contained both H_2 and H_2O. This suggests that Co–Ce–Mn catalysts deactivation for CO-PROX was caused by CO_2 in the feed gas, whereas H_2 and H_2O had little influence on CO removal over Co–Ce–Mn catalysts.

3.2. FTIR of the deactivated sample

The FTIR spectrum of the deactivated Co–Ce–Mn catalyst is shown in Fig. 2. At high wave-number, the broad band at around 3400 cm^{-1} is due to H-bound hydroxyl groups. The strong bands at 567 and 663 cm^{-1} are indicative of the existence of Co_3O_4 spinel oxide in the deactivated catalyst as suggested in references [22–24]. The band at 567 cm^{-1} is associated with OB_3 vibrations in the spinel lattice, where B denotes Co^{3+} in an octahedral position, and the band at 663 cm^{-1} is attributed to the ABO_3 vibrations, where A denotes Co^{2+} in a tetrahedral position.

There are two broad adsorption bands at 1490 and 1380 cm^{-1} and a weaker band at 1050 cm^{-1} in the spectrum. The bands at 1490 and 1380 cm^{-1} can be attributed to C–O stretching of $CO_3{}^{2-}$ ions [25,26]. The band at 1050 cm^{-1} is assigned to horizontally adsorbed CO_2 on the catalyst surface or metal–oxygen stretching of coordinatively unsaturated metal ions and surface oxygen atoms [27]. These results confirm the accumulation of CO_2 on the deactivated cata-

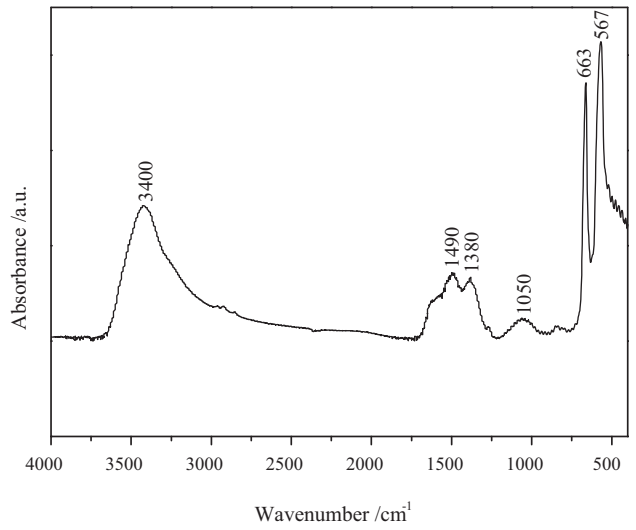

Fig. 2. FTIR spectrum of deactivated Co–Ce–Mn catalyst.

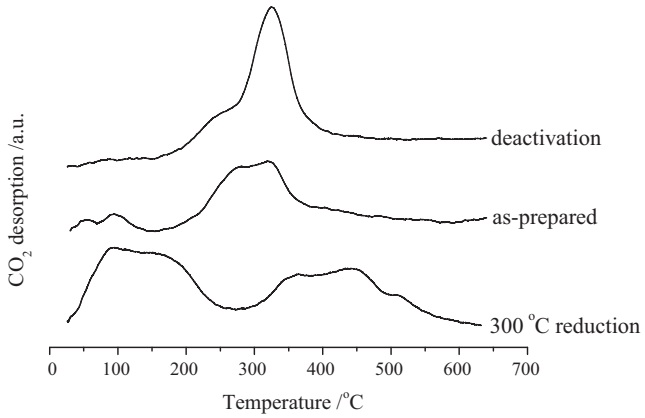

Fig. 3. CO_2-TPD profiles of the fresh and reduced catalysts with CO_2 adsorption pretreatment and the deactivated catalyst.

lysts, which may be responsible for the large impact of CO_2 on the stability of Co–Ce–Mn catalysts.

3.3. CO_2-TPD

Fig. 3 presents CO_2-TPD results for Co–Ce–Mn samples after different pretreatments. The fresh catalyst pretreated with CO_2 showed two small peaks at temperatures <100 °C and a strong peak at ~300 °C. The two small peaks can be attributed to the desorption of weakly adsorbed CO_2 (linear or shearing) and the high-temperature peak to the desorption of carbonates or strongly adsorbed CO_2 (horizontal) [28,29]. The CO_2 desorption peaks for the reduced catalyst were shifted to higher temperature compared to the fresh catalyst. The reduction pretreatment led to the reduction of some cobalt ions from Co^{3+} to Co^{2+} (see the TPR results below). This suggests that the valence state of cobalt has a significant influence on CO_2 desorption and a higher valence state favors CO_2 desorption. The area of the low-temperature peaks is much greater for the pre-reduced sample than for the fresh catalyst, indicating that the reduced catalyst can adsorb much more CO_2 than the fresh sample. This may be attributed to that the reduced sample can offer electrons to CO_2, which favors CO_2 adsorption [30–32].

For deactivated catalysts, low-temperature TPD peaks could hardly be observed, suggesting that weakly adsorbed CO_2 probably has little influence on CO-PROX over Co–Ce–Mn catalysts. The area

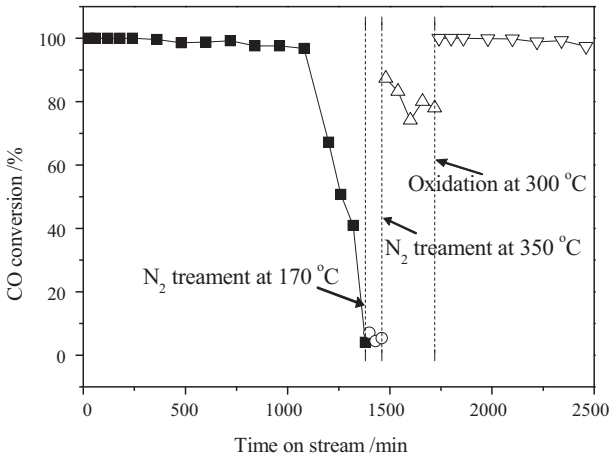

Fig. 4. Variation of CO conversion with reaction time over Co–Ce–Mn catalyst at 170 °C under the space velocity of 80,000 ml h^{-1} g_{cat}^{-1} and in reaction gases of 1 vol.% CO, 1 vol.% O_2, 50 vol.% H_2, 20 vol.% CO_2, 10 vol.% H_2O and N_2. (■) Deactivation with running time; (○) after treated with N_2 at 170 °C for 30 min; (△) after treated with N_2 at 350 °C for 30 min; (▽) after treated with 5% O_2/N_2 at 300 °C for 30 min.

of the peak attributed to carbonate desorption is much greater for the deactivated catalyst than for the fresh and pre-reduced samples, indicating that carbonate accumulation is the cause of deactivation of Co–Ce–Mn catalysts during CO-PROX, in agreement with the FTIR results.

3.4. Regeneration of deactivated Co–Ce–Mn catalysts

If CO_2 accumulation were the only factor causing catalyst deactivation, the deactivated catalyst should be fully regenerated by desorption of CO_2 from the surface of the sample. The results for regeneration of catalysts deactivated in CO-PROX are shown in Fig. 4. After outgassing with N_2 at 170 °C, the deactivated catalyst still exhibited very low activity for CO-PROX. The deactivated sample could be partially reactivated by N_2 degassing at a higher temperature of 350 °C, and this treatment could completely remove CO_2 from the surface of the deactivated catalyst (Fig. 3). When the deactivated catalyst was treated with O_2/N_2 at 300 °C, its activity completely recovered, confirming that the deactivation of Co–Ce–Mn catalysts during CO-PROX is reversible and that ions in the catalysts may have been reduced during deactivation.

3.5. H_2-TPR

Fig. 5 shows the H_2-TPR results for pure Co_3O_4, fresh and deactivated Co–Ce–Mn catalysts. The H_2-TPR behavior of as-prepared Co–Ce–Mn and pure Co_3O_4 was reported in our previous paper [9]. Owing to the low content of MnO_x and CeO_2 in the catalysts and their partial reduction, the relatively smaller reduction peaks for MnO_x and CeO_2 were completely overlapped by those for Co_3O_4. Therefore, the three reduction peaks denoted by α, β and γ should be attributed to Co^{3+} reduction to Co^{2+}, reduction of Co^{2+} not interacting with ceria, and reduction of Co^{2+} interacting with CeO_2, respectively [9].

The α/γ peak area ratio changed from 0.47:1 to 0.29:1 as the Co–Ce–Mn catalyst deactivated during CO-PROX. Although Mn^{n+} might be reduced to Mn^{2+} during the reaction, the α/γ ratio could not decrease to such a low value of 0.29:1, if the valence state of cobalt oxide did not change. This confirms that some of the Co^{3+} ions in the Co–Ce–Mn catalysts were reduced to Co^{2+} in the reaction process. The change in oxidation state of cobalt has seldom been pointed out in the literature, as most researchers have focused

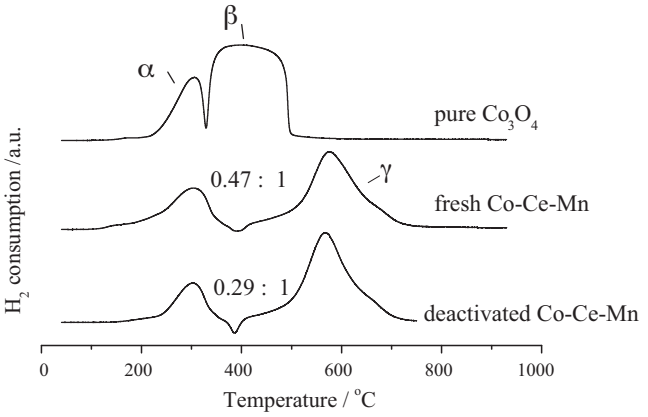

Fig. 5. TPR profiles of pure Co_3O_4, the fresh and deactivated Co–Ce–Mn catalysts.

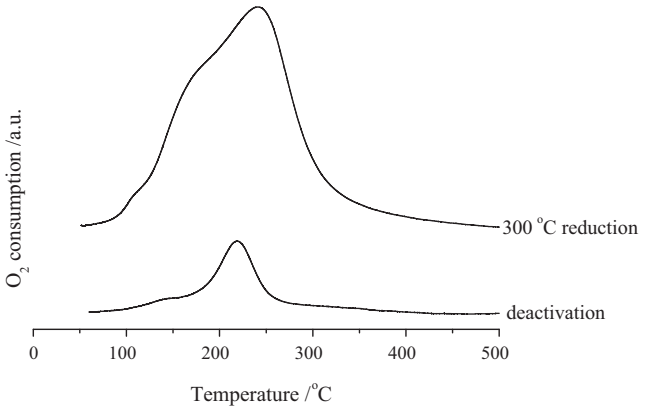

Fig. 6. TPO profiles of reduced and deactivated Co–Ce–Mn catalysts.

on CO_2 accumulation as the cause of catalyst deactivation. Our result also contradicts previous report which suggested that there were no changes in the oxidation state of cobalt during CO low-temperature oxidation [21]. This difference may be attributed to the different reaction conditions. The ratio of O_2:CO in the reactant mixture was 0.6 or 1.5 in [21], so the feeding gases contained enough oxygen for CO oxidation. In the case of this study, O_2 is insufficient since both the oxidation of CO and H_2 consume oxygen competitively. Furthermore, in this work, CO_2 content is 20 times of that in their work [21]. As CO_2 can interact and block the reoxidation of reduced cobalt oxide, some cobalt ions in the catalysts of this study tend to be reduced to lower valence state.

3.6. TPO results

Fig. 6 presents the TPO results for deactivated and 300 °C pre-reduced Co–Ce–Mn catalysts during CO-PROX. The H_2-TPR results indicate that pre-reduction at 300 °C lead to conversion of Co^{3+} to Co^{2+}. The TPO results for the pre-reduced sample show that Co^{2+} was re-oxidized to Co^{3+} at 100–350 °C. Similar reoxidation behavior is evident from the TPO profile of the deactivated Co–Ce–Mn catalyst. The TPO results for the deactivated catalysts suggest that Co^{2+} ions reduced from Co^{3+} during the reaction process can be reoxidized to Co^{3+} in the oxidation regeneration process.

3.7. Activity of Co–Ce–Mn catalysts after different pretreatments

Fig. 7 shows that pretreatments significantly affect the activity of Co–Ce–Mn catalysts. The catalyst pretreated with 5%O_2/N_2 at 300 °C exhibited very high activity for CO-PROX during the whole

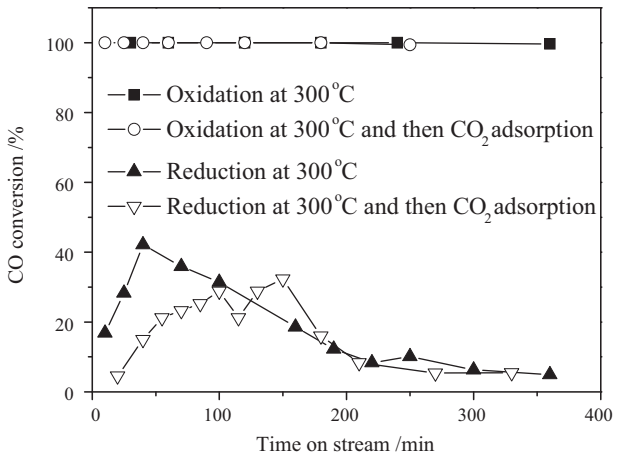

Fig. 7. The activity of Co–Ce–Mn catalyst with different pretreatments for CO PROX. Reaction temperature: 170 °C; space velocity: 80,000 ml h^{-1} g_{cat}^{-1}; Reaction gas: 1 vol.% CO, 1 vol.% O_2, 50 vol.% H_2, 20 vol.% CO_2, 10 vol.% H_2O and N_2.

reaction period. Even when the pre-oxidized catalyst was treated in a flow of CO_2 before activity tests, it was still very active. By contrast, pre-reduction treatment resulted in a significant decrease in activity and CO conversion only reached 42.2%. Since pre-reduction with H_2/Ar reduces Co^{3+} to Co^{2+} (see the H_2-TPR results), it can be deduced that Co^{2+} is less active for CO oxidation and Co^{3+} in Co_3O_4 is essential for the high activity, in agreement with the literatures [12,15,33].

CO conversion over the pre-reduced Co–Ce–Mn catalyst increases with time in the initial stage and then slowly decreases, regardless of whether the catalyst was treated with a CO_2 flow or not. The increase in CO conversion is probably due to partial reoxidation of Co^{2+} to Co^{3+} by O_2 in the reaction gas, whereas CO_2 accumulation on the catalyst surface and a decrease in Co^{3+}/Co^{2+} ratio should be responsible for the decrease in conversion. Carbonated cobalt may be formed along with CO_2 accumulation with the reaction time, and cobalt carbonates are more difficult to be reoxidized. Thus, both the Co^{n+} oxidation state and CO_2 accumulation have a great impact on CO removal from H_2-rich gases.

For the pre-reduced catalyst, CO_2 treatment leads to a decrease in CO conversion. This may result from the adsorption of CO_2 molecules on the catalysts preventing O_2 adsorption and reoxidation of Co^{2+}. For the pre-oxidized catalyst, samples treated with CO_2 exhibited the same catalytic performance as those without CO_2 treatment. This suggests that different oxidation states of cobalt show different CO_2 adsorption/desorption behaviors: oxidized Co^{3+} ions are resistant to deactivation by CO_2 adsorption, whereas Co^{2+} ions are readily occupied by CO_2.

4. Discussion

It has been proposed that CO_2 or H_2O leads to deactivation of cobalt oxide catalysts for CO oxidation [15–19,34]. In the present study, however, only CO_2 in the feeding gas had an impact on CO removal over Co–Ce–Mn catalysts. The presence of H_2O in the reaction gas had little influence on the catalytic activity. This may be due to the higher reaction temperature in this study, which favors H_2O desorption from the catalyst surface.

The accumulation of carbonates and the resulting blockage of active sites should be one reason for the deactivation of Co–Ce–Mn catalysts during CO-PROX, since CO_2 in the feeding gas led to an obvious decrease in CO conversion and adsorbed CO_2 was detected on the deactivated catalyst by FTIR and CO_2-TPD. So far, most

researchers have focused on CO_2 adsorption on the deactivation of cobalt oxide and attributed the deactivation to CO_2 accumulation on the catalyst surface. However, we think that this is not the only reason for Co–Ce–Mn deactivation during CO-PROX, otherwise the deactivated catalyst would be fully regenerated by N_2 treatment at 350 °C which causes carbonate decomposition or CO_2 desorption.

The other reason proposed here for catalyst deactivation is reduction of Co^{3+} active sites. It has been agreed that Co^{3+} in Co_3O_4 is responsible for the high activity of cobalt oxide-based catalysts for CO oxidation [9,15,33]. Our TPR and TPO results indicate that some of the Co^{3+} ions were reduced to Co^{2+} in the deactivated catalyst. Thus, reduction of Co^{3+} ions in the reaction process results in a loss of activity, and oxidation treatment of the deactivated catalyst can regain its high activity for CO-PROX.

It has been proposed that CO oxidation over cobalt oxide catalysts follows a redox mechanism. CO species adsorbed on cobalt sites react with the oxygen atoms around cobalt ions to produce CO_2, which leads to the reduction of Co^{3+} to Co^{2+}. The reduced cobalt ions can then be reoxidized to Co^{3+} by oxygen from the gas phase or additives such as ceria. However, if CO_2 cannot be desorbed from cobalt sites timely, it will transform to carbonates as a more stable state, which affects the activity of the cobalt oxide. In the present study, CO_2-TPD results demonstrate that CO_2 adsorption occurs more readily on Co^{2+} than on Co^{3+}, and it is much more difficult for CO_2 to desorb from Co^{2+} than from Co^{3+}. The occupancy of Co^{2+} sites in cobalt oxide by CO_2 would prevent the adsorption of O_2 on Co^{2+} sites and make Co^{2+} oxidation difficult. In summary, Co^{3+} ions are the key active sites. In the CO-PROX reaction process, Co^{3+} is reduced to Co^{2+}. However, Co^{2+} sites tend to be occupied by CO_2, which blocks the regeneration of Co^{3+} via $Co^{2+} \rightarrow Co^{3+}$. Thus, the redox recycle is broken and the catalyst is deactivated.

5. Conclusions

Co–Ce–Mn catalysts exhibit low stability for CO-PROX, so further insights into the deactivation mechanism are of great significance. In the present study, a deactivation framework is proposed. Co^{3+} ions in Co_3O_4 are responsible for the high activity for CO-PROX, and Co^{3+} is not prone to adsorb CO_2. In the reaction process, Co^{3+} can be reduced to Co^{2+} which tends to adsorb CO_2. The Co^{2+} sites occupied by CO_2 are difficult to be oxidized, preventing the regeneration of Co^{3+} via $Co^{2+} \rightarrow Co^{3+}$. Thus the redox recycle is broken and the catalyst is deactivated. In other words, carbonate accumulation around Co^{2+} ions and the reduction of Co^{3+} ions during reaction cooperatively result in the deactivation of Co–Ce–Mn catalysts.

Acknowledgments

The financial support of this work by Hi-tech Research and Development Program of China (863 program, Granted as Nos. 2006AA05Z115 and 2007AA05Z104), National Natural Science Funding of China (20976121) and the Cheung Kong Scholar Program for Innovative Teams of the Ministry of Education (No. IRT0641) are gratefully acknowledged.

References

[1] S.M. Hwang, O.J. Kwon, S.H. Ahn, J.J. Kim, Chem. Eng. J. 146 (2009) 105.
[2] G. Avgouropoulos, J. Papavasiliou, T. Tabakova, V. Idakiev, V. Ioannides, Chem. Eng. J. 124 (2006) 41.
[3] C. Galletti, S. Specchia, G. Saracco, V. Specchia, Chem. Eng. J. 154 (2009) 246.
[4] H. Igarashi, T. Fujino, M. Watanabe, J. Electroanal. Chem. 391 (1995) 119.
[5] H.F. Oetjen, V.M. Schmidt, U. Stimming, F. Trila, J. Electrochem. Soc. 143 (1996) 3838.
[6] G. Avgouropoulos, T. Ioannides, Appl. Catal. A 244 (2003) 155.
[7] Y. Teng, H. Sakurai, A. Ueda, T. Kobayashi, Int. J. Hydrogen Energy 24 (1999) 355.
[8] Q. Guo, Y. Liu, React. Kinet. Catal. Lett. 92 (2007) 19.
[9] Q. Guo, Y. Liu, Appl. Catal. B 82 (2008) 19.
[10] Q. Guo, M.L. Wu, Y. Liu, X. Bai, Chin. J. Catal. 28 (2007) 953.
[11] Y.Z. Wang, Y.X. Zhao, C.G. Gao, D.S. Liu, Catal. Lett. 125 (2008) 134.
[12] J.J. Shao, P. Zhang, X.F. Tang, B.C. Zhang, W. Song, Y.D. Xu, W.J. Shen, Chin. J. Catal. 28 (2007) 163.
[13] J.Y. Luo, M. Meng, X. Li, X.G. Li, Y.Q. Zha, T.D. Hu, Y.N. Xie, J. Zhang, J. Catal. 254 (2008) 310.
[14] Q. Guo, Y. Liu, Chem. Lett. 37 (2008) 1274.
[15] M. Kang, M.W. Song, C.H. Lee, Appl. Catal. A 251 (2003) 143.
[16] P. Thormählen, E. Fridell, N. Cruise, M. Skoglundh, Appl. Catal. B 31 (2001) 1.
[17] D.A.H. Cunningham, T. Kobayashi, N.K. Haruta, M. Haruta, Catal. Lett. 25 (1994) 257.
[18] F. Grillo, M.M. Natile, A. Glisenti, Appl. Catal. B 48 (2004) 267.
[19] I. Gamboa Mutuberría, J.M. Guil, R. Paniego, Berichte der Bunsengesellschaft für physikalische Chemie 97 (1993) 77.
[20] J. Jansson, E. Skoglundh, E. Fridell, P. Thormählen, Top. Catal. 16–17 (2001) 385.
[21] J. Jansson, A.E.C. Palmqvist, E. Fridell, M. Skoglundh, L. Osterlund, P. Thormahlen, V. Langer, J. Catal. 211 (2002) 387.
[22] Y.Z. Wang, Y.X. Zhao, C.G. Gao, D.S. Liu, Catal. Lett. 116 (2007) 136.
[23] St.G. Christoskova, M. Stoyanova, M. Georgieva, D. Mehandjiev, Mater. Chem. Phys. 60 (1999) 39.
[24] R.N. Singh, J.P. Pandey, N.K. Singh, B. Lal, P. Chartier, J.F. Koenig, Electrochim. Acta 45 (2000) 1911.
[25] M.J. Pollard, B.A. Weinstock, T.E. Bitterwolf, P.R. Griffiths, A.P. Newbery, J.B. Paine, J. Catal. 254 (2008) 218.
[26] G. Busca, R. Guidetti, V. Lorenzelli, J. Chem. Soc. Faraday Trans. 86 (1990) 989.
[27] S.H. Zhong, H.S. Li, J.W. Wang, Chin. J. Fuel Chem. Technol. 27 (1999) 602.
[28] L.G. Tejuca, A.T. Bell, J.L.G. Fierro, M.A. Pena, Appl. Surf. Sci. 31 (1988) 301.
[29] J.W. Wang, Y. Shao, S.H. Zhong, Chin. J. Catal. 19 (1998) 305.
[30] J.C. Tully, Adv. Chem. Phys. 42 (1980) 63.
[31] G. Ertl, B. Bunsenges, Phys. Chem. 86 (1982) 425.
[32] J.W. Wang, S.H. Zhong, Chin. Prog. Chem. 10 (1998) 374.
[33] X.W. Xie, Y. Li, Z.Q. Liu, M. Haruta, W.J. Shen, Nature 458 (2009) 746.
[34] D.A.H. Cunningham, T. Kobayashi, N. Kamijo, M. Haruta, Catal. Lett. 25 (1994) 257.